



Investigation on Failures of Composite Beam and Substrate Concrete due to Drying Shrinkage Property of Repair Materials

Rashmi Ranjan Pattnaik¹

Received: 19 January 2015 / Accepted: 9 May 2017 / Published online: 29 May 2017
© The Institution of Engineers (India) 2017

Abstract A Finite Element Analysis (FEA) and an experimental study was conducted on composite beam of repair material and substrate concrete to investigate the failures of the composite beam due to drying shrinkage property of the repair materials. In FEA, the stress distribution in the composite beam due to two concentrate load and shrinkage of repair materials were investigated in addition to the deflected shape of the composite beam. The stress distributions and load deflection shapes of the finite element model were investigated to aid in analysis of the experimental findings. In the experimental findings, the mechanical properties such as compressive strength, split tensile strength, flexural strength, and load–deflection curves were studied in addition to slant shear bond strength, drying shrinkage and failure patterns of the composite beam specimens. Flexure test was conducted to simulate tensile stress at the interface between the repair material and substrate concrete. The results of FEA were used to analyze the experimental results. It was observed that the repair materials with low drying shrinkage are showing compatible failure in the flexure test of the composite beam and deform adequately in the load deflection curves. Also, the flexural strength of the composite beam with low drying shrinkage repair materials showed higher flexural strength as compared to the composite beams with higher drying shrinkage value of the repair materials even though the strength of those materials were more.

Keywords Deterioration · Concrete repair · Bonding strength · Slant shear bond strength · Drying shrinkage

Introduction

Shrinkage of a repair material can cause failure. If the repair material shrinks excessively and cracks then any protective properties or load bearing characteristics, in the case of structural repair, will be lost. To ensure durability of repaired areas, repair materials must exhibit low shrinkage [1]. The selection of an appropriate repair material is a function of the type of structure, existing stress conditions at the location of the repair, environmental exposure conditions, and the time constraints placed on the repair operations [2]. However, in practice the selection of repair material is most often based on achieving certain minimum compressive strength in a short duration, so that the structure can be put into immediate service. While meeting the short term strength requirements for opening the repaired structure for service in a short period does not ensure long-lasting and durable repair. In particular, the present practice does not consider the long-term properties of the repair materials, which can be significantly different from the properties measured at early ages. Also, the emphasis in existing specifications for selection of repair materials on the properties of repair material alone and does not give consideration to the properties of the substrate concrete. In this regard, there can be a significant mismatch in properties such as modulus of elasticity, shrinkage potential, coefficient of thermal expansion and response to environmental exposure of the repair materials and that of the substrate concrete, leading to bond-related failures [3]. Substantial advances have been

✉ Rashmi Ranjan Pattnaik
rashmirpattnaik@gmail.com

¹ Department of Agricultural Structure, Civil and Environmental Engineering, College of Agricultural Engineering & Technology, Orissa University of Agriculture and Technology, Bhubaneswar, India

made in the field of repair materials, while the industry still has an unacceptable high level of defects and failures of concrete repairs [4].

Drying shrinkage of the repair material induces tensile stresses at the interface between repair and substrate materials, potentially causing failure. By the time repair materials are cast over the substrate concrete, the substrate concrete would have already gone through numerous cycles of drying and wetting, and consequently would exhibit only minimal reversible shrinkage. Drying shrinkage values of repair materials in excess of 0.05 and 0.1% at 30 days are considered to represent moderate and high levels of drying shrinkage, respectively, that can potentially result in premature failures [5].

In this research, the failures of repair were investigated using a composite beam similar to the work done by researchers [6] under third point loading as shown in Fig. 1, and using modified ASTM C78 test procedure [7]. A finite element model of the composite section was studied to investigate the influence of variations in the properties of the repair and substrate materials on the stress distribution and deformation across the composite specimen. Load–deflection curves of the composite section with different properties of repair material were developed to compare with the experimental findings.

Research Significance

This research study investigates the drying shrinkage property of repair materials using composite beam of repair material and substrate concrete. This study shows how drying shrinkage property of repair material influences the

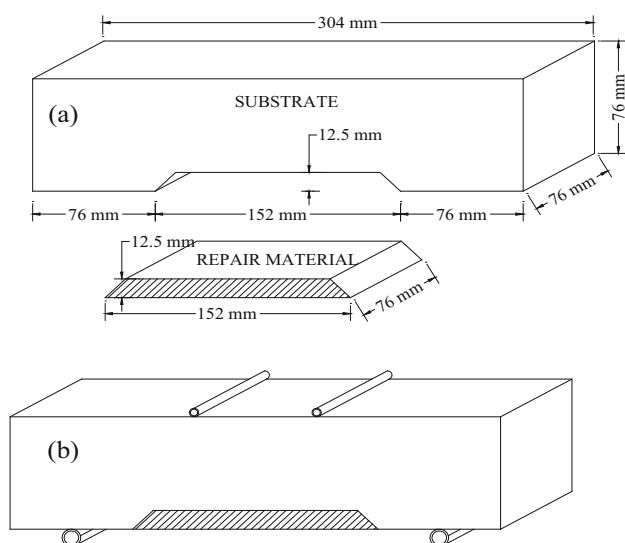


Fig. 1 **a** Dimensions of substrate concrete beam and repair, **b** composite beam, bottom support locations and top point of loadings

concrete repair failure. To achieve durable repair, it is necessary to consider the factors affecting the selection of repair materials as parts of a composite system. The findings of this research can help in selecting repair materials for durable concrete repairs.

Finite Element Program

To assess the stress distribution and deflection in the composite beam due to shrinkage of repair materials, a Finite Element Model (FEM) was developed in STAAD. Pro program. The model consists of substrate material and repair material represented as different Modulus OF Elasticity (MOE) as shown in Fig. 2. The objectives of the FEM investigation were to study-

1. The relative stress distribution in the repair material and the substrate material due to load and shrinkage under different modular ratio (i.e. ratio of modulus of elasticity of repair material to the modulus of elasticity of substrate material).
2. To plot the deflected shape and the load deflection curves of the composite beams in different modular ratio.

The objective of FEM analysis was to study the relative stress distribution in the composite beam of substrate concrete and repair materials. Therefore, the interface between substrate and repair material were not modeled with different material properties.

The composite section was modeled with three and four-noded plate elements of thickness 76 mm in STAAD. Pro program. Two point loads of 20 kN each were applied at the top, analogous to the support and loading condition of ASTM C78 procedure. The support conditions were pinned at one end and roller support at the other end. The deflections were measured at the middle of the beam in different modular ratio of the composite beam.

The MOE of the substrate material was assumed 21.7 GPa (3.15×10^6 psi), and the modulus of elasticity of repair materials were varied from 15.2 to 28.2 GPa to achieve a modular ratio ranging from 0.7 to 1.3 respectively, keeping the poisson's ratio of both materials at 0.17.

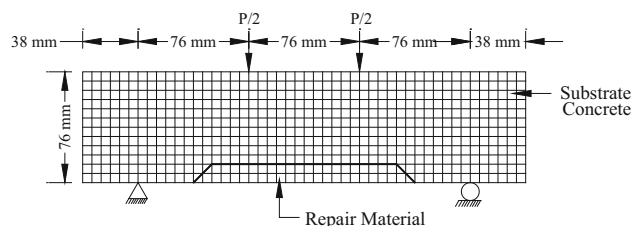


Fig. 2 Finite element model of the composite beam

However, any difference in MOE magnitude would show similar sort of stress distribution in the composite section. The results of FEM analysis, stress concentrations and the deformed shapes were investigated under following three load cases.

1. Two concentrate point load of 20 kN each
2. 0.05% shrinkage load in the repair materials
3. Combined load of two concentrated loads and 0.05% shrinkage load.

Experimental Program

Experimental Test Materials

In this investigation, eight different rapid setting cementitious repair materials were selected from the approved list of South Carolina Department of Transportation (SCDOT), USA for use on repairs of concrete bridge decks. The materials were selected in such a way that the compressive strength of four repair materials were above the compressive strength of substrate concrete and four of them were below the strength of substrate concrete. The precise composition of these repair materials was proprietary and therefore unknown. The specific instructions provided by the manufacturer were followed in preparation of a batch of the repair material for casting on the test specimens. In addition to the repair materials, Type-I Portland cement was used along with natural sand and coarse aggregate (9.5 mm maximum aggregate size) in preparing the substrate concrete specimens in a mix proportion as shown in the Table 1 [3].

The experimental program consisted of casting 72 substrate concrete prism specimens in 76 mm × 76 mm × 305 mm (3-in. × 3-in × 12-in) steel prism molds that were fitted with a specially designed inset to create a notch at the bottom of the substrate concrete for the repair materials. The dimensions of the test specimen are shown in the Fig. 1a. Four batches of concrete were prepared to cast for twelve notch and six full beam sections per batch. In addition, six 76 mm × 152 mm (3-in. × 6-in) cylinders

were prepared from the same batch to determine the compressive strength of the concrete in two different curing conditions. Each of these tests was conducted on three test specimens in air-dry and moist curing conditions. The mixture proportions and the mixing procedure were identical in preparing substrate specimens in each of the eight batches. Six substrate specimens from the same batch were used in bonding a given repair material to avoid any variability. The proportions of the substrate concrete used in preparing the notch and full beams are shown in the Table 1.

Experimental Test Methods

1. *Setting time* Repair materials are most often selected based on setting time. Quicker the repair material sets faster the repaired section opened for service. Setting time of the repair materials were measured using Vicat needle as per modified ASTM C191 standard practice of method-A (manually operated). The initial time of setting was determined as the elapsed time required to achieve a penetration of 25 mm and the final setting as the total elapsed time when the needle does not sink visibly into the paste.
2. *Compressive strength* The compressive strength of the repair materials were determined using 50-mm (2-in) cube as per the ASTM C 109 standard practice, since the repair materials were primarily mortars. The compressive strengths of substrate concrete were determined using 76 mm × 152 mm (3-in × 6-in) cylinder as per ASTM C39. The cubes of the repair materials were tested in compression at 8 h, 24 h, 14 days, and 28 days. The cylinders of the substrate concrete were tested at 35 and 63 days, corresponding to the day of casting and 28 days of repair materials, respectively. Cubes and cylinders of repair materials and substrate concrete were tested for their compressive strength alongside the testing of composite sections from the same batch.
3. *Drying shrinkage* The drying shrinkage of the repair materials were measured on 304 mm (12-in) length and 25 mm × 25 mm (1-in × 1-in) cross sectional area of prismatic section as per ASTM C157 standard practice. The specimens were moist cured for 3 days prior to testing. The readings were taken at 7, 14, 21 and 28 days, and drying shrinkage percentage was measured with reference reading of at 4 days after the moist curing.
4. *Slant shear bond strength* The bond strength of the repair materials is determined using the standard ASTM C 882 test procedure which is the extension of the Arizona slant shear test [8]. In this test procedure, the repair material is bonded to a substrate

Table 1 Substrate concrete proportions, per m³

Items	Quantity
Water-cement ratio, based on SSD aggregate	0.40
Mix water	172 kg
ASTM type-I Portland cement	362 kg
Coarse aggregate (oven dry)	1068 kg
Fine aggregate (oven dry)	753 kg
High range water reducer	780 ml/100 kg

mortar specimen on a slant elliptical plane inclined at 30° angle from vertical to form a $76 \text{ mm} \times 152 \text{ mm}$ (3-in. \times 6-in) composite cylinder as shown in Fig. 3.

Before the repair material is bonded to the substrate mortar, the slant surfaces of the substrate mortar specimen were prepared by sandblasting and dry brushing. The test was performed by determining the compressive load required to fail the composite cylinder and the bond strength is calculated as $[\text{Max Load}]/[\text{Area of Slant Surface}]$.

5. *Split tensile strength* The split tensile strength of the repair materials and the substrate concrete were determined on $76\text{-mm} \times 152\text{-mm}$ (3-in. \times 6-in) cylinders as per the ASTM C 496 test method. The split tensile strengths of repair materials were measured at 1 h, 24 h, 14 days, and 28 days. Whereas the split tensile strengths of the substrate concretes were measured at 35 and 63 days, corresponding to day of casting and 28 days of the repair materials.
6. *Flexural Strength of composite beam and substrate concrete* In this test method, concrete prisms 304 mm (12-in) in length with a cross-section of $76 \text{ mm} \times 76 \text{ mm}$ (3in \times 3in) were cast as per standard ASTM C 78 test procedure. The span length of the prism should be at least three times its depth as shown in Fig. 1. The load was applied through two points that are located at one-third of the span length from each support. As a result, the maximum stress is induced in the middle-third of the prism. The flexural strength determined from this procedure is referred to as Modulus of Rupture.

The composite prism for evaluating the compatibility of repair material with substrate concrete was fabricated to the same dimensions as the control prism, with the exception that a wide-mouthed notch 152 mm (length) \times 76 mm (width) \times 12.5 mm (depth) was cast into the bottom of the

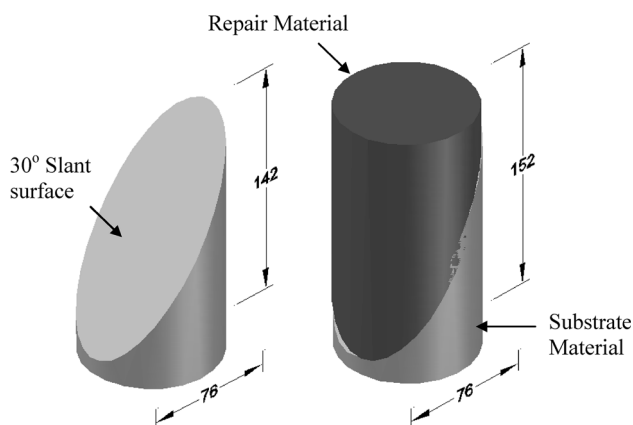


Fig. 3 Dimension of composite section for slant shear bond-strength, mm

composite prism using a 3-dimensional inset (Fig. 1). After de-molding, the prisms were moist cured for 28 days, and then the wide-mouthed notch areas were textured using sand blasting and dry brushing. The rough surface textured substrate specimens were air-dry cured for 7 days before patching the notched area with the repair materials. Half of The composite sections were de-molded next day and moist cure for 28 days, and other half kept for air-dry cure for 28 days. After 28 days, the composite sections were tested in third point loading beam test, as per ASTM C78 test procedure. Also, at the time of testing for flexural strength, the deflections in the prisms at the center were measured to examine the mode of failure with the deformation. For substrate concrete (consisting of 9.5 mm maximum aggregate) prisms of 304 mm (12-in) length and $76 \text{ mm} \times 76 \text{ mm}$ (3-in \times 3-in) cross-sectional area were used. The flexural strength of the substrate concrete was tested at 63 days, corresponding to 28 days test of repair materials.

Results and Discussions

Finite Element Analysis

It was observed in the finite element analysis that the distribution of major principal stress in the composite section changes under two concentrate loads as a function of the modular ratio as shown in the Fig. 4. As the modular ratio deviates from 1.0, the stress concentration in the composite section is either higher or lower at the bottom fibers as compared to the composite section of modular ratio equal to 1 (i.e. control substrate concrete prism). For instance, when the modular ratio is 1.3, higher tensile stress concentration occurs on the substrate as well as repair material. This indicates that when the repair material is significantly stronger than the substrate concrete the failure preferentially occurs at center. This is because the repair material cannot deflect to the same extent as substrate concrete (that has a lower stiffness), provided that the bond between the two materials is adequate to transfer the load to the repair material at the bottom. However, when the modular ratio is 0.70 (i.e. the repair material is weaker than the substrate material), the lower tensile stress concentration occurs on the repair material and the substrate. In this case, depending on the bond strength, the failure occurs either at center or at the edge of the repair. Incidentally, it was observed in the experimental findings that when the repair material is weaker, the bond strength required to transfer the load is lower in magnitude. This situation forces the failure to occur preferentially at the middle third instead of edge [3].

Similarly, due to 0.05% shrinkage in the repair material, the distribution of major principal stress in the composite

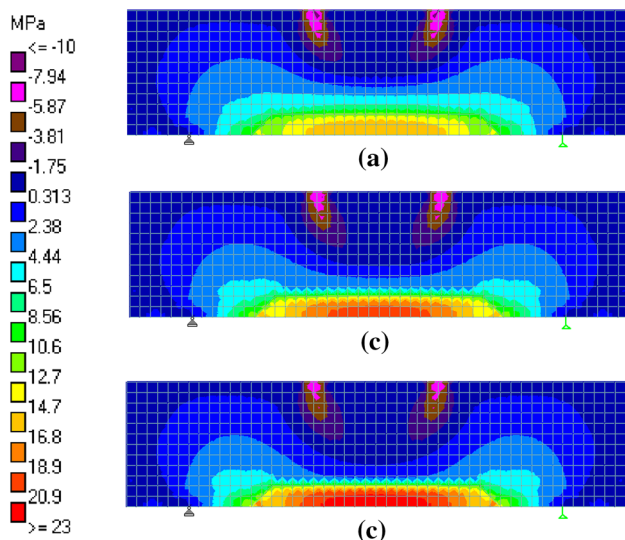


Fig. 4 Major principal stress distributions due to point loads. **a** M.R. = 0.7, **b** M.R. = 1.3, **c** M.R. = 1.0

section changes as a function of the modular ratio as shown in Fig. 5. It was observed; when the repair material was significantly stronger than the substrate concrete the major principal stress distribution was higher at the interface between repair material and substrate material. The durability of such cases depends on the bond strength between the two materials to transfer the load to the substrate material.

Figure 6 shows the load–deflection curves of the composite sections in the FEM analysis. It can be observed in Fig. 6 that as the stiffness of the repair material increases, the slope of the curve increases. For instance, in case of composite beam with a modular ratio of 1.3, the slope of load–deflection curve is higher than that of a composite

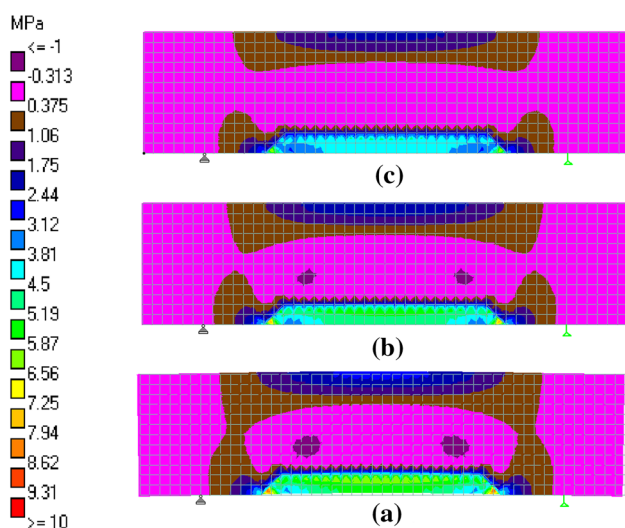


Fig. 5 Major principal stress distributions due to shrinkage. **a** M.R. = 0.7, **b** M.R. = 1.0, **c** M.R. = 1.3

beam with a modular ratio of 1.0 and 0.7. This implies that at a particular load, the higher stiffness repair material deflects less as compared to a repair material that has lower or similar stiffness as substrate material; provided the bond is adequate to transfer the load.

Experimental Findings

1. *Setting time* Table 2 shows the final setting time of the repair materials. It can be observed all the repair materials except repair material D, set within 40 min from mixing.
2. *Compressive strength* Table 3 shows the compressive strength of the repair material. These values are the average of the compressive strengths of three cubes. All the compressive strengths were found increasing from 8 h to 28 days except the repair material E, which showed lower compressive strength at 14 and 28 days. Further investigation revealed that the repair material E loses its strength in moist curing. This is also noticed by the researchers [9] due to certain ingredient present inside the repair material.
3. *Drying shrinkage* Fig. 7 shows the drying shrinkage of the repair materials. These values are the average of three specimens. It can be observed that the repair materials D and G showed high drying shrinkage (i.e. >0.1% at 28 days, Emmons et al. 1993). The repair materials A, B and C, which have moderate drying shrinkage value (i.e. >0.05% at 28 days). It can be observed that the repair materials E and H showed low drying shrinkage (i.e. <0.05% at 28 days).
4. *Bond strength of repair materials* In this study, two classes of bond strength observed (a) Minimum bond strength (calculated as per ASTM C 882), and (b) Actual Bond Strength. If the failure occurred on the slant surface, the actual bond strength is same as the minimum bond strength. However, if the failure surface is not on the interface, the bond strength as per the ASTM C 882 calculation represents minimum bond strength.

It can be observed from the results in Table 4 that in the repair materials A, B, C and D that the failure in the composite cylinder occurred in the substrate material, instead on the interface. It was also observed that the failure of the composite cylinders occurs in the substrate, if the compressive strength of repair materials is greater than the substrate materials. In case of repair material E, the failure occurs in the repair material because of lower compressive strength than the substrate material (Table 4). When the compressive strength is close to the compressive strength of substrate mortar, in this situation, it is evident from observing the data in Table 4 that the failure occurs

Fig. 6 Load deflection curves of composite beams in FEM analysis

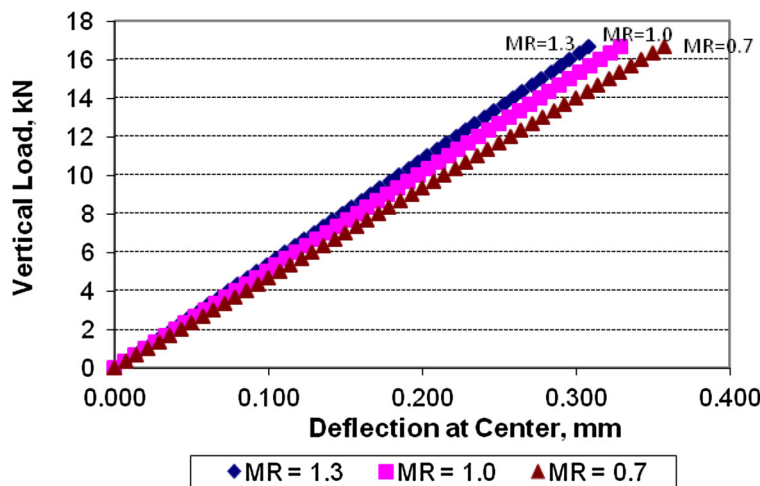


Table 2 Setting time of the repair materials

Repair materials	Final setting time, min
A	19
B	20
C	26
D	240
E	10
F	20
G	28
H	40

Table 3 Compressive strength of repair materials

Repair materials	Compressive strength, MPa			
	8-h	24-h	14-days	28-days
A	40.0	52.4	63.7	65.0
B	30.3	36.2	63.5	63.2
C	37.9	41.1	59.3	66.6
D	6.7	22.4	80.0	80.9
E	44.6	47.8	29.8	30.6
F	23.2	30.0	49.2	55.2
G	26.2	38.6	42.6	43.6
H	26.8	35.5	43.5	45.6

on the interface between the repair material and substrate mortar. It can be observed from the data that the composite cylinders did not fail on the interface because of the improved bond strength. These results validate the findings of previous studies on surface-finish and strength of substrate influence the slant shear strength [10, 11].

5. *Split tensile strength* Table 5 shows the split tension of the repair materials. These values are average of three specimens. Repair Materials G and H recorded very low tensile strength at 1 h.

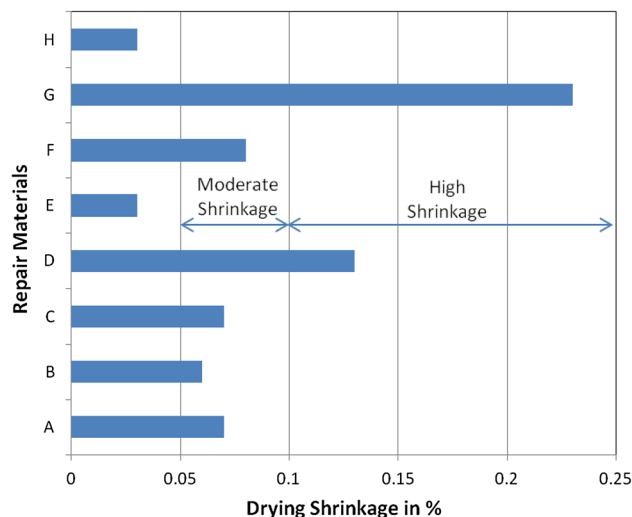


Fig. 7 Results of drying shrinkage of the repair materials

Table 4 28 days slant shear strength of repair materials

Repair material	Bond strength (as ASTM C 882, MPa)	Actual bond strength, MPa	Failure mode
A	21.8	–	Substrate
B	21.3	–	Substrate
C	21.2	–	Substrate
D	21.4	–	Substrate
E	15.4	–	Repair material
F	20.2	20.2	Interface
G	21.1	21.1	Interface
H	17.8	17.8	Interface

6. *Flexure strength of composite beam* Tables 6 and 7 shows the 28-days results of the compressive strength, flexural strength, compressive strength ratio and the failure pattern of the composite beams. In addition, the

Table 5 Split tensile strength of repair materials

Repair materials	Split tension, MPa			
	1-h	24-h	14-days	28-days
A	1.4	4.9	5.3	5.3
B	1.3	3.6	5.0	5.4
C	2.4	4.6	5.4	6.1
D		5.3	6.2	7.1
E	2.2	2.8	2.5	2.9
F	1.9	3.8	4.8	5.4
G	0.1	2.6	5.5	4.9
H	0.1	3.1	3.8	4.2

Table 6 Flexural strength of composite beams in moist curing

Repair material	Compressive strength, MPa		Flexural strength, MPa	Comp. strength ratio	Failure pattern
	RM	Substrate			
A	93.5	56.0	7.1	1.67	Compatible
B	95.6	56.2	7.9	1.70	Incompatible
C	77.6	52.8	5.5	1.47	Incompatible
D	68.8	55.9	5.9	1.23	Incompatible
E	51.8	52.9	6.0	0.98	Compatible
F	58.3	50.3	8.6	1.16	Incompatible
G	52.2	50.2	7.4	1.04	Compatible
H	45.6	56.3	5.5	0.81	Compatible

Table 7 Flexural strength of composite beams in Air-dry curing

Repair material	Compressive strength, MPa		Flexural strength, MPa	Comp. strength ratio	Failure pattern
	RM	Substrate			
A	76.2	68.0	6.8	1.12	Compatible
B	76.0	67.9	6.1	1.12	Compatible
C	64.6	63.3	5.8	1.02	Incompatible
D	65.8	67.8	6.2	0.97	Compatible
E	65.1	63.2	7.8	1.03	Compatible
F	42.5	59.0	5.1	0.72	Incompatible
G	46.2	59.2	5.0	0.78	Incompatible
H	45.0	68.2	6.5	0.66	Compatible

corresponding load versus deflection curves of these specimens in the flexure test are shown in the Figs. 8 and 9.

In the present investigation, the average compressive and the split tensile strength of the substrate concrete at

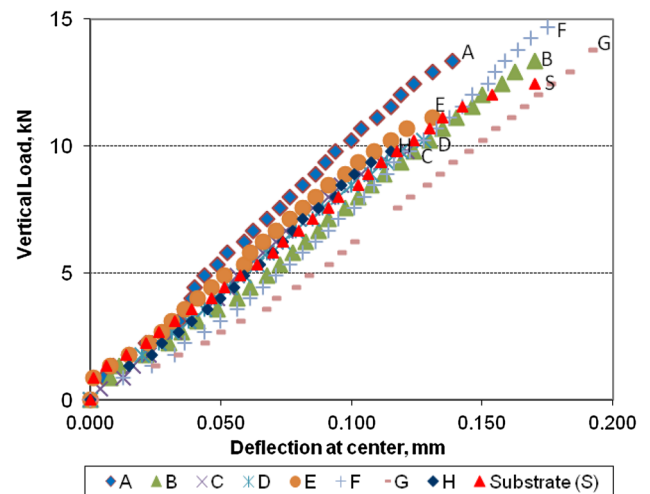


Fig. 8 Load deflection curves of composite beams in moist curing

35 days were found to be 48 and 4.1 MPa (6960 and 595 psi), respectively. It was observed that in the subsequent 28 days during which the composite sections were cured, the substrate concrete registered only an average additional 4.4 MPa (638 psi) increase in compressive strength and 1.1 MPa (160 psi) in split tensile strength. In contrast, test specimens of repair materials cast alongside the composite section exhibited a rapid gain in compressive strength and split tensile strength within 28 days, ranging from 31 and 2.9 MPa to 81 and 7 MPa, respectively.

It is apparent from observing the data in Tables 3 and 5 that depending on the specific repair material; significant difference exists between the properties of the repair material and the substrate at any given age. This disparity in strengths can be expected to influence the failure mode.

In conducting the flexure tests of composite beams, two different modes of failures were observed as shown in Fig. 10. Figure 10a shows the failure at the center of the composite section indicating a compatible failure of the repair material [6]. Figure 10b shows the failure of the composite section failure at edge of the notch section indicating an incompatible failure of the repair material.

In this study, load–deflection curves were plotted to assess the compatibility between the repair and substrate concrete materials for durable repair [3].

It can be observed from Tables 6 and 7 that even though the compressive strength ratios of repair materials A, B, C and E in Table 7; A, B, C, D, and F in Table 6, were greater than 1.0, some of these repair materials showed either higher or lower slopes in the load–deflection behavior of composite beams in the flexure test, depending on the specific curing condition. For instance, repair materials C in Figs. 8 and 9, and D in Fig. 8, showed lower slopes and others showed equal or higher slopes. The repair materials those were not deforming adequately with the

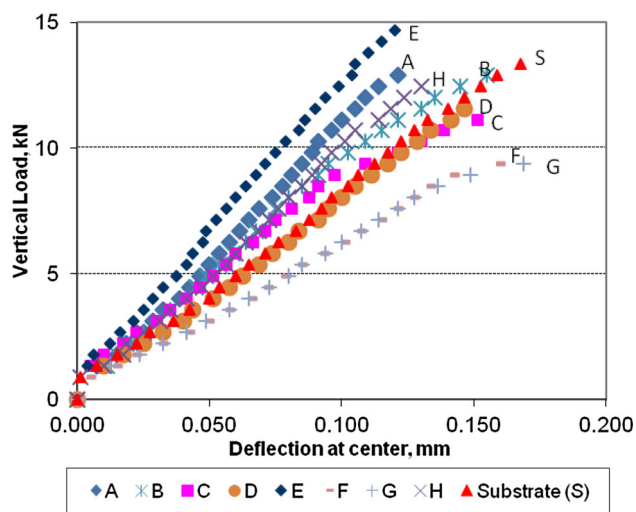


Fig. 9 Load deflection curves of composite beams in Air-dry curing

substrate beam, even though compressive strengths were more than substrate concrete, showed lower slope in load-deflection and showed incompatible failures [3].

It can be observed from Tables 6 and Table 7 that the repair material compressive strength ratio less than 1.0 were failing either at the middle-third portion or at the edge. For instance repair materials F and G in the Table 7, the compressive strength ratios were 0.72 and 0.78 respectively, the failure occurred at the edge. This indicates that these materials were not compatible with the substrate concrete.

The composite section beam with repair materials B, C, D and F in Table 6; having compressive strength ratios more than 1.0 and high split tensile strength of the repair materials, indicate that these sections have more compressive strength and tensile strength than a substrate concrete beam. The failure pattern of the composite section shows that these materials are incompatible with the substrate concrete as failures occurred at the end of the repair

as shown in Fig. 10b due to high strength of repair material.

Effect of Drying Shrinkage

It was observed in the FEM analysis as shown in the Fig. 5, due to shrinkage of the repair materials the composite beam deform upward. Whereas, due to the concentrated load, the composite beam was deformed downward, as shown in Fig. 4. The combined effect of concentrated load and shrinkage of repair materials deformed the composite beam downward as shown in Fig. 11, which is less than the deformation due to the concentrate loads alone. It was also observed that the vertical (Y) deflection was maximum in the case of repair materials with lower strength.

Generally, the repair mortars applied to hardened concrete substrates have a tendency to shrink on drying. As a result of restraint provided by the substrate at the interface and/or the periphery for an enclosed patch repair, drying shrinkage cannot proceed freely, and the problem is further compounded if the repaired structure is subjected to an aggressive environment. As a result, the developments of various stress components were observed in the FEM analysis, which can lead to premature failure of the repair.

For instance, the repair material G which has a very high drying shrinkage value, more than 0.2% of drying shrinkage value, showed an incompatible failure in the flexure test as shown in the Table 7. It has also showed lower slope in the load deflection curve of composite beam as shown Fig. 9. This is because the stress concentration is more in the interface between substrate and repair material as observed in the finite element analysis.

All the repair materials except repair materials E and H, showed moderate to high drying shrinkage value. Therefore, depending upon the bond strength these repair materials showed compatible or incompatible failures. For instance, the repair materials A, B and D showed adequate

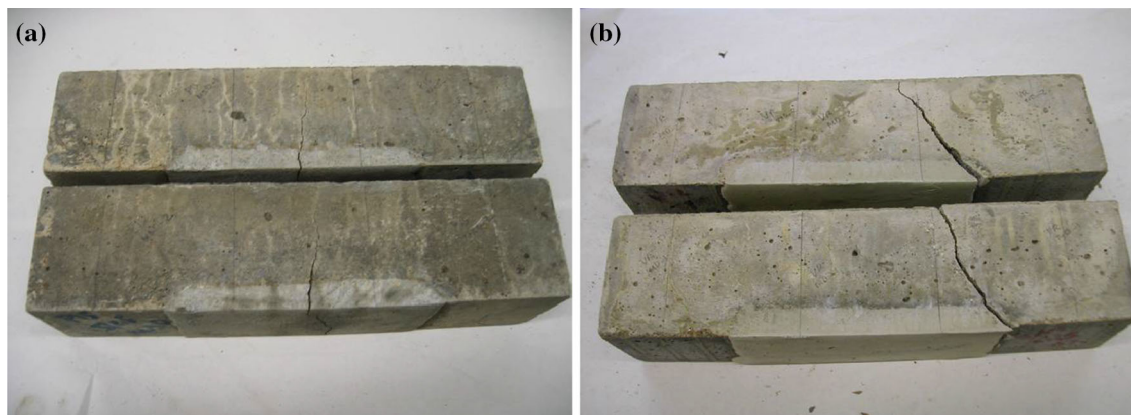


Fig. 10 Failure patterns of composite beam. **a** Failure at center, **b** failure at the edge of repair

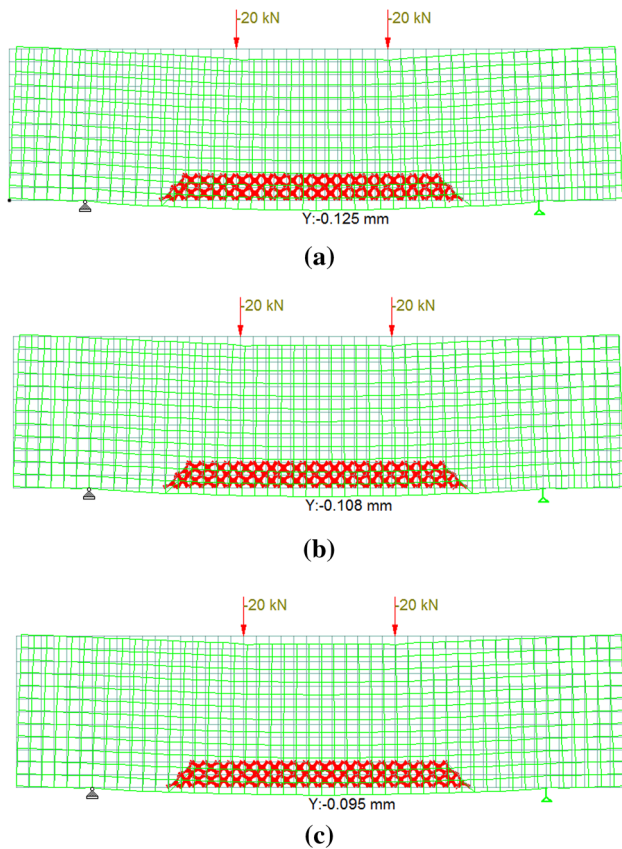


Fig. 11 Maximum vertical (Y) deflections due to combined point load and shrinkage. **a** M.R = 0.7, **b** M.R = 1.0, **c** M.R = 1.3

deformation and failed at the center as a compatible failure due to good bondage. Whereas, the repair materials C and F has showed incompatible failures as shown in the Table 7.

It was observed in the Fig. 9, the drying shrinkage of the repair materials E and H have very low values which showed higher slope in the load deflection curve of the composite beams, even though the repair materials E and H were having lower or close to the value of compressive strength and split tensile strength of the substrate concrete, contrasting to the higher strength repair materials. It was also observed in Table 7 the flexural strength of the composite beam with repair materials E and H in the air-dry cure condition showed higher flexural strength because of low drying shrinkage values even though the tensile strength of the repair materials were lower than the substrate concrete.

Conclusion

Based on the results from the finite element analysis and the experimental program it can be concluded that the use of a high strength repair material is inappropriate for selection of repair materials. Instead, the low drying shrinkage value of the repair material is preferable in selecting repair material for a durable concrete repair. Due to low shrinkage the flexural strength of the composite beam increases and the repair material deform adequately with the substrate concrete. Therefore, the author suggests the new generation repair materials must include a shrinkage compensation action to reduce the drying shrinkage for durable concrete repair.

References

1. M.H. Decter, C. Keeley, Durability of concrete repair—importance of compatibility and low shrinkage. *Constr. Build. Mater.* **11**(5–6), 267–273 (1997)
2. A.M. Vaysburd, P.H. Emmons, N.P. Mailvaganam, J.E. McDonald, B. Bissonnette, Concrete repair technology—a revised approach is needed. *Concr. Int.* **26**(1), 59–65 (2004)
3. R.R. Pattnaik, P.R. Rangaraju, Analysis of compatibility between repair material and substrate concrete using simple beam with third point loading. *J. Mater. Civ. Eng. ASCE* **19**(12), 1060–1069 (2007)
4. J.E. McDonald, A.M. Vaysburd, P.H. Emmons, R.W. Poston, K. Kesner, in *Selecting durable repair materials: performance criteria—Summary*, Concrete international, vol. 24, issue 1 (ACI, 2002), pp. 37–44
5. P.H. Emmons, A.M. Vaysburd, J.E. McDonald, in *A rational approach to durable concrete repairs*. Concrete international, vol. 15, issue 9 (ACI, 1993), pp. 40–45
6. L. Czarniecki, A. Garbacz, P. Lukowski, J.R. Clifton, “*Polymer composites for repairing of Portland cement concrete- compatible project*”, NISTIR 6394 (Building and Fire Research Laboratory, NIST, Gaithersburg, 1999), p. 20899
7. R.R. Pattnaik, P.R. Rangaraju, Investigation on flexure test of composite beam of repair materials and substrate concrete for durable repair. *J. Inst. Eng. (India): ser. A* **95**(4), 203–209 (2014)
8. J.D. Kreigh, Arizona slant shear test. *ACI J.* **73**, 372–373 (1976)
9. Q. Yang, B. Zhu, X. Wu, Characteristics and durability test of magnesium phosphate cement-based material for rapid repair of concrete. *Mater. Struct.* **33**, 229–234 (2000)
10. A. Momayez, M.R. Ehsani, A.A. Ramezaniapour, H. Rajaie, Comparison of methods for evaluating bond strength between concrete substrate and repair materials. *Cem. Concr. Res.* **35**(2005), 748–757 (2005)
11. R. Saldanha, E. Júlio, D. Dias-da-Costa, P. Santos, A modified slant shear test designed to enforce adhesive failure. *Constr. Build. Mater.* **41**, 673–680 (2013)